Journal of Machine Engineering, Vol. 9, No. 4, 2009

robotic assembly
best-fit algorithm
aero-engine components

Nirosh JAYAWEERA[1]
Phil WEBB[2]
Craig JOHNSON[3]

A NOVEL APPROACH FOR THE ASSEMBLY OF FABRICATED AERO-ENGINE COMPONENTS

Currently the manufacturing of aero-engine intercase is primarily a single piece titanium casting and has slightly deteriorated material properties as compared to sheet metal parts and has long manufacturing lead time. As an alternative solution to above problems, the VITAL (Environmentally Friendly Aero Engines) project aims to design, manufacture and test the critical technologies required to develop new type of clean and low noise aero engines by developing innovative technical solutions to reduce the engine's weight, thereby reducing both fuel consumption and CO2 emission. This requires the fabrication of small and weight optimised parts which will be automatically manipulated, welded, assembled and inspected in a flexible fabrication cell. The paper introduces a novel techniques for compensating the deformation that occur in aero-engine fabricated components and potential component handling errors using standard industrial robots, an advanced end-effector, mathematical processing, non-contact metrology systems and cell control system. The system described in this paper uses in-process measurement sensors to determine the component's exact location prior to the assembly operation. The core of the system is a set of algorithms capable of best fitting measurement data to find optimal assembly of components.

1. INTRODUCTION

Aero-engine industries are continuously setting goals for environmental impact and industry competitiveness for future commercial air transport. Currently the main challenges facing the aero-engine industry is the reduction of aircraft engine noise and Carbon Dioxide emissions. The VITAL (Environmentally Friendly Aero Engines) project is an integrated project funded under the European Union Sixth Framework programme that aims to make aircraft engines greener, less noisy and more fuel efficient [1]. One way of achieving this is to move from a cast manufacturing method to a fabrication method for large engine structures [2]. This can reduce the engine's weight thereby reducing fuel consumption and hence Carbon Dioxide emissions.

[1] Department of Mechanical, Materials and Manufacturing Engineering, University of Nottingham, UK
[2] Department of Systems Engineering and Human Factors, University of Cranfield, UK
[3] Rolls-Royce plc, Derby, UK

Conventionally automated assembly of these structures has been limited due to high cost associated with the complex fixture and the significant manual labour input required. This paper describes a novel approach to the fabrication of such structure and its application to the assembly of fabricated aero-engine components. Currently the majority of automation solutions used in the aerospace industries is based around large dedicated fixed systems. These are inflexible, have long manufacturing lead time and can lead to capital bottlenecks. One way of introducing flexibility is by incorporating robots. Background literature suggested that there has been limited work on the use of flexible robot based systems in aerospace assembly applications. All these systems required accurate positioning and fixturing of the components within the cell to overcome the inherent flexibility of robot structures. However a number of articles do describe robotic applications in the aerospace industry and demonstrate that there is a significant amount of interest in the adoption of external metrology systems to improve the capability of robotic systems. Most of the existing research such as the assembly of wing structures [3,4], the TI^2 system for the manufacturing of airframe subassemblies [5] and metrology assisted robot calibration [6], automated assembly of fuselage skin panels [7] and assembly of aero-engine components [8] utilise metrology systems specifically laser tracker, photogrammetry, laser radar, laser stripe scanners and vision systems to provide the assembly and manufacturing operations. These installations have all supported greater levels of automation.

The majority of the work published on robotic installations in the aerospace industry is based on drilling and riveting applications for aero-structure sub-assemblies and automated robotic assembly of aero-structure components and little work has been reported on the assembly of fabricated aero-engine components. However a number of articles [9,10,11,12] do describe the development of new technologies necessary for achievement of environmental objectives of future aero engines using heat management, improved combustion, active systems and improve core components. The paper describes an automated solution for the assembly of fabricated aero-engine components by integrating a standard industrial robot, non-contact metrology systems, a mathematical processing toolbox and a cell control system.

2. METHODOLOGY

To perform the assembly of fabricated components a standard industrial robot and two 'off the shelf' non-contact metrology systems were used. One metrology system was mounted on the robot's end-effector to find true edge positions relative to the robot BASE coordinate system and the other was mounted statically within the robot's work volume to find component true edge profiles relative to the robot TOOL coordinate system. The BASE coordinate system is the coordinate system for the robot which is located at the base of the manipulator affixed to the non-moving part of the robot and the TOOL coordinate system is affixed to the end of any tool or gripper on the robot. The acquired data could then be processed using a mathematical algorithm to calculate the true relationship between the robot's Tool Centre Point (TCP) and the part and counterpart. The system proposed calculates the actual relationship between the robot TCP and component to be measured and uses this relationship to generate the required robot programs by manipulating a pre-programmed robot path. This optimises the performance of the robot used since they are locally calibrated to each other and since the robot operates in a relatively small working area relative to the workpiece it ensures that maximum repeatability and accuracy are achieved. If the part cannot be placed in the exact position required embedded software performs a 'best-fit' operation relative to features on its counterpart, along with an overall tolerance check, to ensure that the part can be assembled within the required specifications. This methodology is capable of compensating for the deformation that occurs in aero-engine fabricated components and potential component handling errors since parts are measured after they have been picked up. This approach provides a significant cost savings by eliminating the need for precise fixtures and complex end-effectors.

3. CELL CONSTRUCTION

To test the proposed methodology a demonstrator cell was constructed which consisted of Comau S2 robot, pneumatic end-effector, MTF seam finder, MXS cross sensor, aero-engine sector components and modular fixtures as shown in Fig. 1. Comau S2 robot has an articulated, six axes anthropomorphic structure with a large working envelop. Its maximum wrist load capacity is 8kg and the Repeatability is ± 0.1 mm. To identify and localise the components a Meta MXS cross sensor (mounted on the robot's end effector) and a Meta MTF seam finder (mounted statically within the robot's work volume) were used. The Meta MTF single stripe sensor is relatively low cost, lightweight and contains a CCD camera and a single laser diode. The laser acts as a structured light source and produces a stripe on the surface under the sensor. The MTF control unit processes the picture from the camera and the software and uses the settings from the seam type to divide the stripe into lines that form that seam. From the position of the lines it can detect the location of the seam.

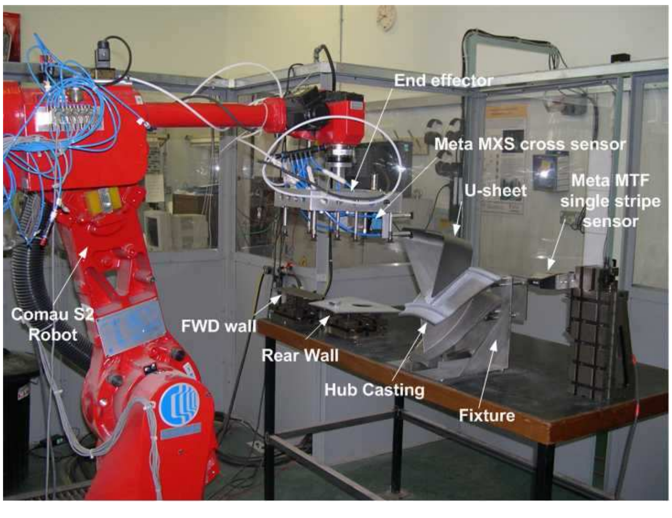

Fig 1. Experimental setup

Measurements from the picture are then converted into measurements in millimetres to give the seam's position under the sensor. MXS cross sensor is also operates in same principle as described above and uses two laser stripes to generate positional data on features of interest. An end-effector was manufactured and integrated with the robot and incorporated both a gripping and sensing systems. The developed end-effector was capable of handling all the sector components. Mathematical processing of the measurement data was performed using algorithms built using MATLAB software.

Cell communication was via Ethernet, and serial communication. Ethernet was chosen due to its capability to support the transfer of large volume of data through FTP file transfer protocols. A serial port was used to transfer the laser data to the robot controller. This integrated system is capable of passing data between all the system elements through a control PC and a diagram of the cell resources and architecture is shown in Fig. 2. In the work described here a fabricated titanium sector was considered to be a single entity which approximates to $1/10^{th}$ of the complete aero-engine intercase. A fabricated sector consists of assembly of a U-sheet, Rear T-Box Wall (RW) and Forward T-Box Wall (FWD) on to a hub-casting as illustrated in Fig. 3.

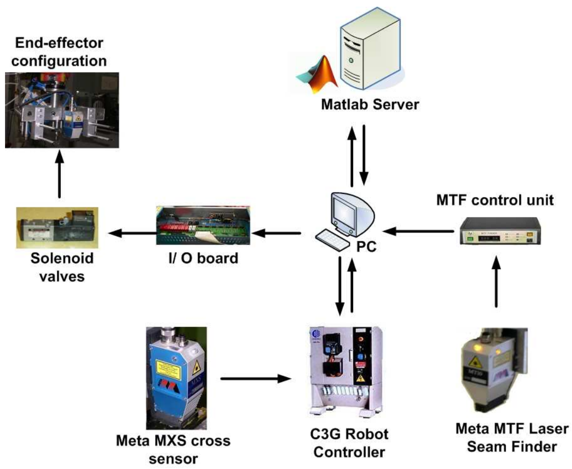

Fig. 2. Cell control architecture

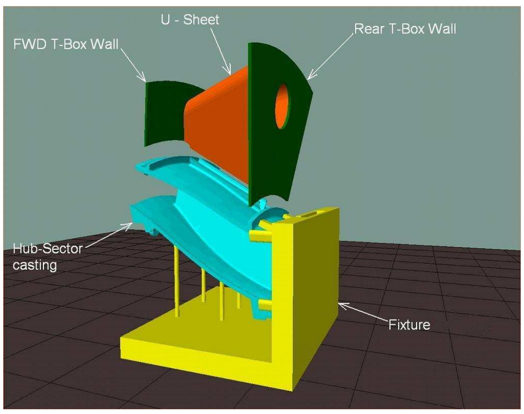

Fig. 3. A fabricated sector

Assembly of the U-sheet was not performed due to dimensional variability and deformation from previous manufacturing processes but the process was proved using an aluminium component of the same dimensions. During the experiments the U-sheet was fixed on to the hub-casting using Araldite adhesive.

4. CELL OPERATION

The first stage of the assembly operation was to measure the hub-casting by taking measurement points along its edges using a Meta MXS sensor. For this geometry 7 scanning points for each curved edge and 5 scanning points for each side edge were taken. The resulting laser offset values and robot positions were then sent back to the control PC for data manipulation. The acquired data was used to find the true edge profiles in 3D space. These calculated true positions were used to generate 3D ‘best-fit’ lines and 3D ‘best-fit’ curves to find the intersection points (point 1 to 4) and further processes to find optimal drop off positions of rear and FWD T-box walls relative to robot’s BASE coordinate system as illustrated in Fig. 4. These drop-off positions and endpoints were stored in the form of a text file to be available for further processing.

In stage 2, the U-Sheet was manually attached to the casting before commencing the rest of the assembly process. For the U sheet geometry eight points were measured around four straight edges and obtained laser offset values and robot positions were sent back to the control PC for data manipulation relative to the robot BASE coordinate system. The obtained measurement data was used to calculate true positions and further processed to find U-point 1 and U-point 2 as illustrated Fig. 5. These points were also stored in the form of text files to be available for further processing.

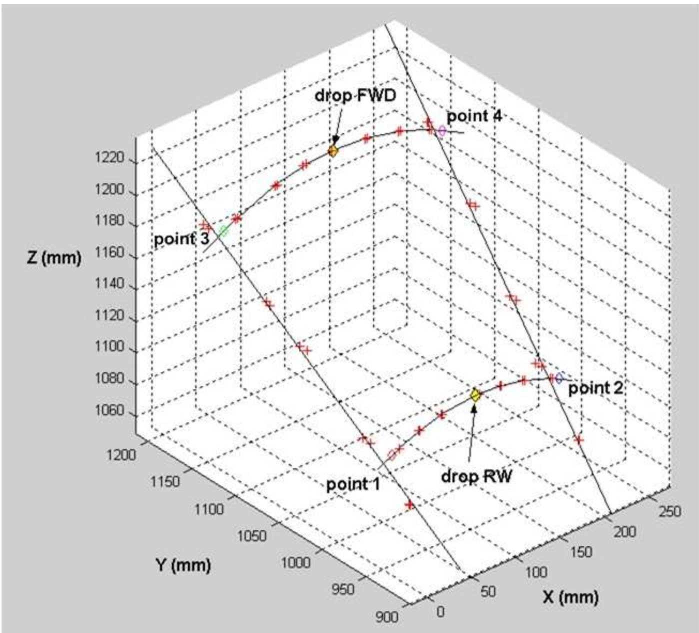

Fig. 4. Calculation of drop-off positions on the hub-casting

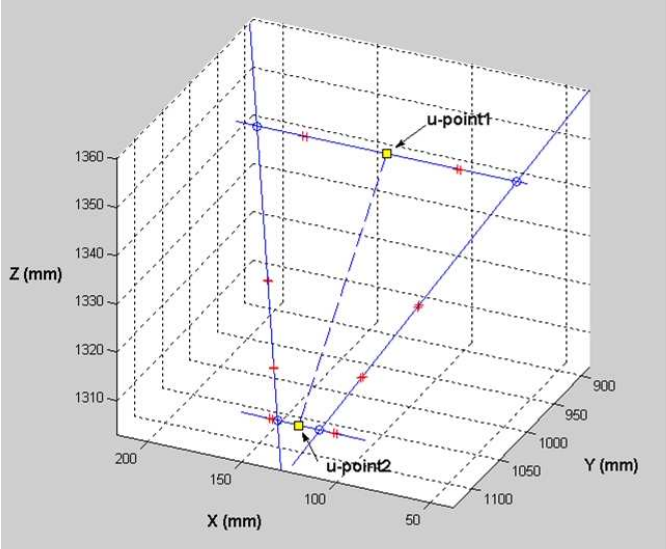

Fig. 5. U-sheet calculation

In stage 3, the RW and FWD geometries were scanned using a Meta MXS sensor in such a way that 3 scanning points for each straight edge and 5 scanning points for each curved edges were taken and obtained laser offset values and robot positions were then sent back to the control PC. The data obtained was used to find its true edge profiles in 3D space. The generated true positions were then used to calculate 3D 'best-fit' lines and 3D 'best-fit' curves to find the optimal part pick up points of RW and FWD walls relative to robot's BASE coordinate system. The calculation of the part pick-up positions is only required as a one-off calculation as any variation of component location can be compensated for during the next stage of the assembly operation.

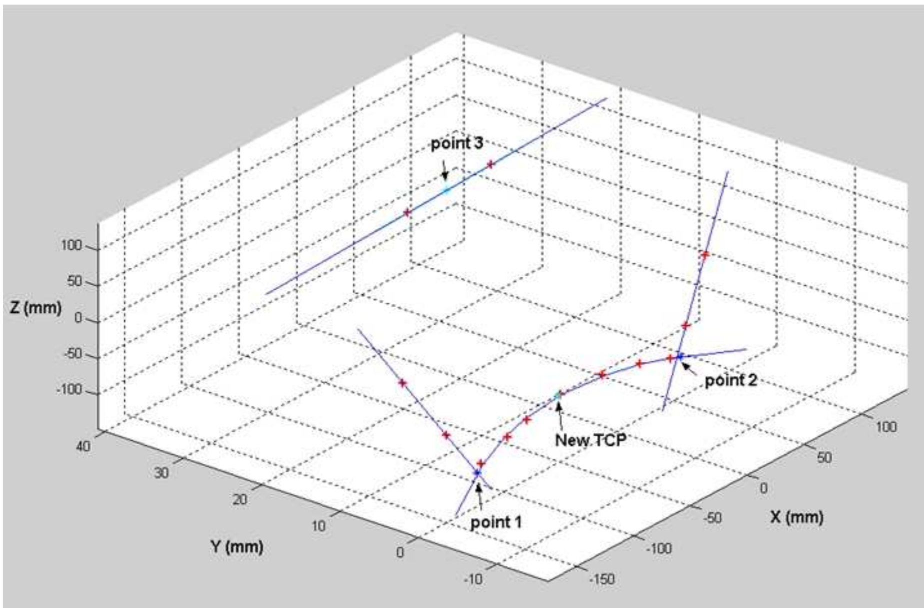

Fig. 6. Calculation of the new TCP point on the RW

In stage 4, each part is picked up and move to the static MTF laser position to scan edge profiles by moving the robot through a set of fixed increments. For the RW and FWD wall geometries 7 scanning points for curved edges and 2 scanning points for each straight edge were taken. At each increment the laser offset values and robot positions are sent automatically to a remote PC. This data was then used to find true edge profiles in 3D space. The true edge positions were subtracted from the robot TCP to find the measured edge positions relative to the robot TOOL coordinate system and further matrix transformations used to find the edge positions relative to the scanning orientation as the relationship between part and robot TCP does not change during robot movement. The data was further processed by generating 3D lines and 3D 'best-fit' curves to calculate intersection points (point1 and point 2), new TCP position, and point 3 as shown in Fig. 6 and 7.

In RW calculation, the obtained points (point 1 and point 2) and points (point 1 and point 2) obtained in stage 1 on the hub-casting were used to calculate XY and XZ angle difference in the Roll, Pitch and Yaw (RPY) coordinate system. The obtained points (new TCP and point 3) in RW and points (drop RW and u-point1) obtained in stage 1 and 2 for hub-casting and u-sheet was used to calculate YZ angular difference in RPY coordinate system. In FWD wall calculations, the obtained points (point 1 and point 2) and points (point 3 and point 4) in stage 1 for hub-casting were used to calculate XY and XZ angle difference in RPY coordinate system.

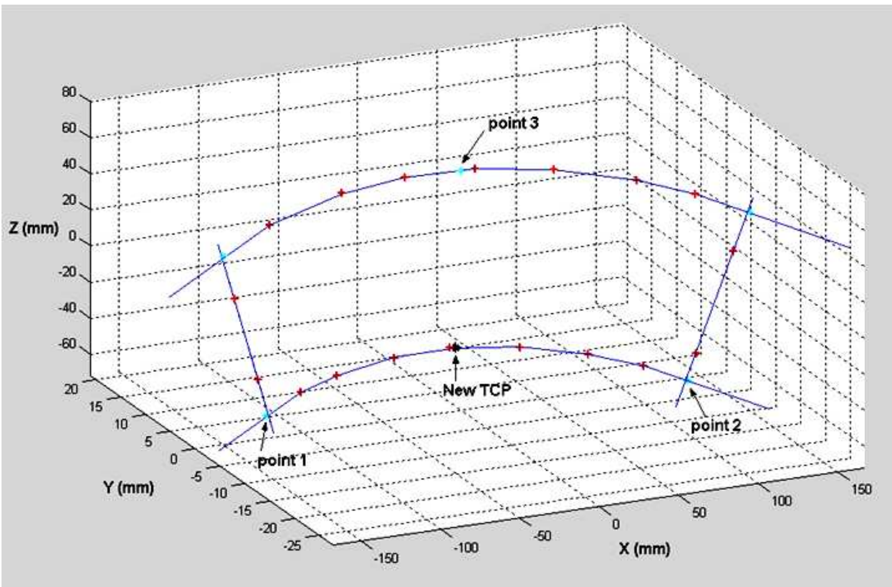

Fig. 7. Calculation of the new TCP point on the FWD

The obtained points (new TCP and point 3) in FWD and points (drop FWD and u-point2) obtained in stage 1 and 2 for hub-casting and u-sheet was used to calculate YZ angular difference in RPY coordinate system. Next, the obtained RPY angles were converted back to Euler angles to find the assembly orientations of forward wall along with the drop-off positions which has already been calculated in stage1.

5. SYSTEM TESTING AND VALIDATION

During setup the Laser TCP was calibrated relative to the robot TCP to provide a reference between the two co-ordinate frames. To test the RW and FWD assembly accuracies 15 experimental trials were performed and the mating surface misalignment between the base of the part and the hub-casting was assessed. Assembly misalignment between RW/FWD and the hub-casting was measured at points ‘a’ and ‘b’ and the notations were illustrated in Fig. 8. This gives a general view of assembly misalignment. The hub-casting edge was selected as the reference edge since it was accurately machined.

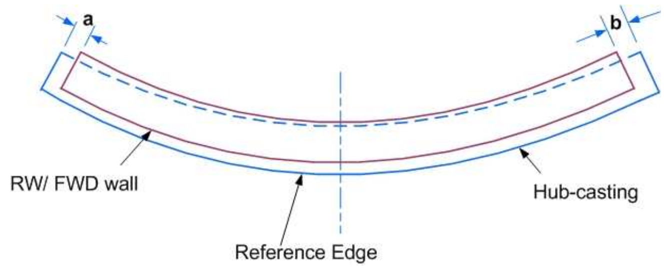

Fig. 8. Generic view of assembly misalignment between RW/FWD wall and hub-casting

Further, the side difference (magnitude of a-b) was calculated and plotted against the number of experimental trials. The resulting measurements from each of the assembly experiments are shown graphically in Fig. 9. It can be seen from Fig. 8 that the side difference falls within 0.5 mm.

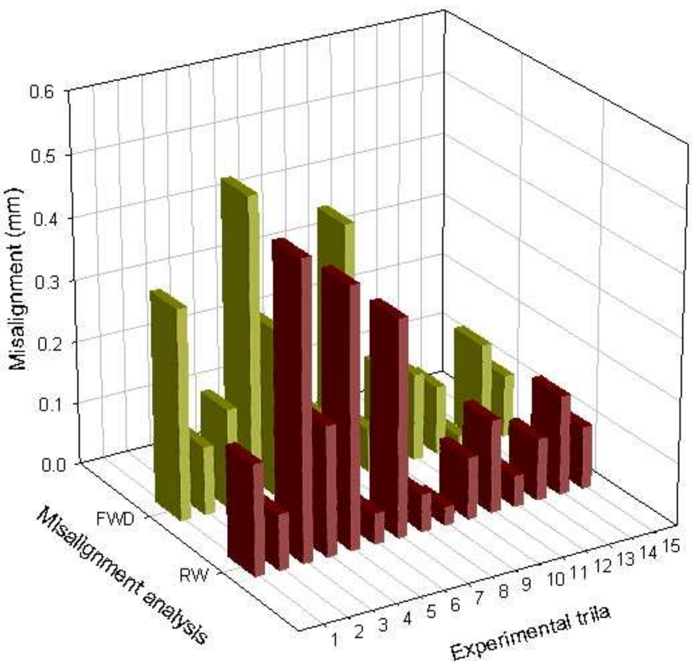

Fig. 9. Component misalignment after assembly

A number of factors can cause inaccuracies in robotic assembly. These include manufacturing tolerances of parts, distortion of components, errors on vacuum gripping, robot errors, robustness of the metrology systems and setting up TCPs. The U-sheet used within this research was dimensionally inaccurate having been distorted during previous manufacturing processes and further distorted whilst manually fixing it on to the hub-casting. Therefore, further research on component manufacturing processes is necessary to improve the dimensional accuracy of the fabricated component to fully evaluate assembly accuracy. Variations of laser offset values were found during scanning trials due to the condition of the machined edges and surface finish of parts. The assembly process can be further improved by using a single stripe sensor mounted on the robot to measure the hub-casting edges instead of the MXS cross sensor.

6. CONCLUSIONS

The paper proposed a novel methodology for the assembly of fabricated aero-engine components where automated assembly has not previously been used. The developed methodology has been evaluated and demonstrated using aero-engine components. The scanning of the part after it has been picked up was very successful providing improved performance and potentially significant cost savings by eliminating the need for precise part loading systems and end-effectors. This paper introduces a technique for compensating for the possible distortions that occurs in aero-engine components. This is an enabling technology that will significantly increase the number of possible applications for robots in the assembly of fabricated components. The developed system reduces the reliance on part holding fixtures and the use of a laser-guided robot ensures that the integrated assembly system is highly flexible and re-configurable.

ACKNOWLEDGEMENTS

This work was funded under European Commission Framework 6 as part of the VITAL integrated project. The authors would like to acknowledge the contribution of Rolls-Royce plc and Volvo Aero Cooperation.

REFERENCES

[1] SJUNNESSON A., FRIDOLF P., MARQUINA F., SPRINGMANN M., 2009, *The VITAL project's approach for reducing weight of turbofan engine structures*, 19th ISABE conference, Montrial , Canada.

[2] WEBB P., JAYAWEERA N., YE C., JOHNSON C., 2008, *Robotic Assembly of Aero-engine Components*, Aerospace Manufacturing and Automated Fastening Conference and Exhibition, North Charleston, South Carolina, USA.

[3] ANDERSON J., 2002, *Advanced Robotic Applications in Aircraft Component Assembly*, Proceeding of Mechatronics, University of Twente, Netherlands.

[4] KAYANI A., JAMSHIDI J., 2007, *Measurement assisted assembly for large volume aircraft wing structures*, 4th International Conference on Digital Enterprise Technology, University of Bath, UK, 426-434.

[5] WEBB P., EASTWOOD S., 2004, *An Evaluation of the TI2 Manufacturing System for the Machining of Airframe Subassemblies*, Journal of Engineering Manufacture, Part B, 218/819-826.

[6] KIHLMAN H., LOSER R., COOKE A., 2004, *Metrology-integrated Industrial Robots – Calibration, Implementation and Testing*, Proceeding of the 35th International Symposium on Robotics, Paris, France.
[7] JAYAWEERA N., WEBB P., 2007,*Automated assembly of fuselage skin panels*, Assembly Automation, 27/4/343-355.
[8] JAYAWEERA N., WEBB P., YE C., JOHNSON C., 2008, *Robotic Assembly of Aero-engine Components*, Journal of Machine Engineering, 8/3/5-16.
[9] WELLS G., MORGAN S., MASSE B., SCHEUGENPFLUG H., 2001, *EEFAE - efficient and environmentally friendly aero engine - technology platform*, Air & Space Europe, 3/3-4/163-165.
[10] LUNDBLADH A., SJUNNESSON A., 2003, Heat Exchanger Weight and Efficiency Impact on Jet Engine Transport Applications, 16th ISABE Conference, Cleveland Ohio, USA.
[11] WILFERT G., KRIEGL B., WALD L., JOHANSSEN O., 2005, *CLEAN - Validation of a GTF High Speed Turbine and Integration of Heat Exchanger Technology in an Environmental Friendly Engine Concept*, ISABE, Munich, Germany.
[12] BOCK S., HORN W., SIEBER J., 2008, *Active Core – A Key technology for more environmentally friendly aero engines being investigated under the NEWAC program*, In 26th international congress of the aeronautical sciences, Anchorage, Alaska, USA.